Published in final edited form as:
Clin Cancer Res. 2010 January 1; 16(1): 184–194. doi:10.1158/1078-0432.CCR-09-1180.

JNK-1 Inhibition Leads to Antitumor Activity in Ovarian Cancer

Pablo Vivas-Mejia[1,2,*], **Juliana Maria Benito**[1,*], **Ariel Fernandez**[3], **Hee-Dong Han**[4], **Lingegowda Mangala**[4], **Cristian Rodriguez-Aguayo**[1,5], **Arturo Chavez-Reyes**[5], **Yvonne G. Lin**[4], **Alpa M. Nick**[4], **Rebecca L. Stone**[4], **Hye Sun Kim**[4], **Francois-Xavier Claret**[5], **William Bornmann**[1], **Bryan TJ. Hennessy**[3], **Angela Sanguino**[1], **Zhengong Peng**[1], **Anil K. Sood**[4,6,7,†], and **Gabriel Lopez-Berestein**[1,6,7,†]

[1] Department of Experimental Therapeutics, University of Texas M. D. Anderson Cancer Center, Houston, TX 77030.

[2] University of Puerto Rico Comprehensive Cancer Center, Rio Piedras, PR 00935.

[3] Department of Bioengineering and Division of Applied Physics, Rice University, Houston, TX 77005.

[4] Department of Gynecologic Oncology, University of Texas M. D. Anderson Cancer Center, Houston, TX 77030.

[5] Department of Systems Biology, University of Texas M. D. Anderson Cancer Center, Houston, TX 77030; Centro de Investigación y de Estudios Avanzados del IPN, Unidad Monterrey,PIIT, 66600 Apodaca NL, Mexico.

[6] Department of Cancer Biology, University of Texas M. D. Anderson Cancer Center, Houston, TX 77030.

[7] Center for RNAi and non-coding-RNA, University of Texas M. D. Anderson Cancer Center, Houston, TX 77030.

Abstract

Purpose—To demonstrate the functional, clinical and biological significance of JNK-1 in ovarian carcinoma.

Experimental Design—Analysis of the impact of JNK on 116 epithelial ovarian cancers was conducted. The role of JNK *in vitro* and in experimental models of ovarian cancer was assessed. We studied the role of WBZ_4, a novel JNK inhibitor redesigned from imatinib based on targeting wrapping defects, in cell lines and in experimental models of ovarian cancer.

Results—We found a significant association of pJNK with progression free survival in the 116 epithelial ovarian cancers obtained at primary debulking therapy. WBZ_4 led to cell growth inhibition and increased apoptosis in a dose dependent fashion in four ovarian cancer cell lines. *In vivo*, while imatinib had no effect on tumor growth, WBZ_4 inhibited tumor growth in orthotopic murine models of ovarian cancer. The anti-tumor effect was further increased in combination with docetaxel. Silencing of JNK-1 with systemically administered siRNA led to significantly reduced

Requests for reprints: Anil K. Sood, Departments of Gynecologic Oncology and Cancer Biology, University of Texas M.D. Anderson Cancer Center, 1155 Herman Pressler, Unit 1362, Houston, TX 77030. Phone: 713-745-5266; Fax: 713-792-7586; asood@mdanderson.org. Gabriel Lopez-Berestein, MD, Department of Experimental Therapeutics, The University of Texas M. D. Anderson Cancer Center, 1515 Holcombe Boulevard, Box 422, Houston, TX 77030; telephone: (713)792-8140; Fax: (713)796-1731; glopez@mdanderson.org. .

*These authors contributed equally to this manuscript

†These authors share senior authorship for this manuscript

tumor weights as compared to non-silencing siRNA controls, indicating that indeed the antitumor effects observed were due to JNK-1 inhibition.

Conclusions—These studies identify JNK-1 as an attractive therapeutic target in ovarian carcinoma and that the re-designed WBZ_4 compound should be considered for further clinical development.

Keywords

JNK-1; Ovarian Cancer; Wrapping defects; Tyrosine Kinase inhibitor; Dehydrons

INTRODUCTION

JNKs or Stress Activated Protein Kinases (SAPK) are members of the Mitogen Activated Protein Kinase (MAPK) family. Of the three isoforms that have been described, JNK1 and JNK2 are ubiquitously expressed while JNK3 is only present in the brain, heart and testes. Controversial effects have been reported for JNKs (1-3). JNKs have been shown to serve as mediators of apoptosis in response to cellular stress (1-7), to sustain cell proliferation, and survival in response to extracellular stimuli such as cytokines (1). JNKs are serine/threonine protein kinases that can be activated by a variety of stimuli including environmental stress (UV and ionizing radiation, heat shock, osmotic or redox shock), inflammatory cytokines and growth factors. Induction by their own phosphorylation, leads to the activation of different transcription factors including c-Jun and JunD. This induction, depending on the cellular context, can have effects at the level of apoptosis, differentiation, survival and carcinogenesis. Based on gene disruption experiments, it was concluded that JNK1 and JNK2 have overlapping functions (8-10). However, Sabapathy et al showed that in fibroblasts, JNK1 has a prominent role in c-Jun activation leading to cell proliferation while JNK2 inhibits cell proliferation by promoting c-Jun degradation in unstimulated cells (11).

Recent findings suggest that JNK mediates oncogenic functions in several cancer types including head and neck, gastric, and breast cancers, and melanoma (12-19), thus it may be an attractive therapeutic target. Gross and colleagues (15) demonstrated that JNK inhibition, mediated by the competitive inhibitor SP600125 or by specific siRNA, inhibited growth of head and neck squamous cell carcinoma *in vitro* and *in vivo* (15). The anti-tumor effects were thought be mediated via effects on both tumor and endothelial cells. Specifically, JNK1 but not JNK2 has been shown to be important in promoting cell survival by controlling cell cycle arrest and apoptosis (12). Little is known about the role of JNK1 in ovarian cancer growth; therefore, we examined the potential of JNK1 as a therapeutic target in the current study. We utilized a novel small molecule inhibitor, WBZ_4, which was designed, synthesized, and characterized by our team to curb the potential for side effects of the original compound, imatinib (20). WBZ_4 was designed to target both c-Kit and JNK1 while avoiding the Abl-kinase. The redesign process was based on comparing the residence time of water molecules that solvate the interfacial aligned residues across known targets of imatinib. Non-conserved sites with low residence time that had a higher propensity to dehydrate (de-wetting hot spots) were used to build blueprints for each target. By adding a methyl group to the original imatinib, we were able to attack a de-wetting hot spot present in C-Kit and JNK1 but absent from BCR-Abl, thereby increasing the specificity of the drug towards the desired targets (20-21). Here, we report on the biological effects of JNK-1 inhibition, both *in vitro* and *in vivo* using experimental models of ovarian cancer.

Materials and Methods

Cells and culture conditions

The human ovarian epithelial cancer cells IGROV1, SKOV3ip1, SKOV3.TR, HeyA8, HEYA8.MDR, A2780PAR, and A2780CP20 cells have been described elsewhere (22-24). All tumor cell lines were regularly screened for Mycoplasma using MycoAlert (Cambrex Bioscience, East Rutherford, NJ) as described by the manufacturer. Cells were maintained in RPMI-1640 medium supplemented with 10% fetal bovine serum (FBS) in 5% CO_2/95% air at 37°C. *In vitro* assays were performed at 70-85% cell density.

Drugs and Reagents

The design and total synthesis of WBZ_4 (*N*-5-[4-(4- methyl piperazine methyl)-benzoylamido]-2-methylphenyl-4-[3-(4-methyl)-pyridyl]-2-pyrimidine amine) has been described previously (21). For in vivo therapy, WBZ_4 and docetaxel (Aventis Pharma, Bridgewater, NJ) were reconstituted in Ca^{2+} and Mg^{2+} free PBS. For *in vitro* testing, docetaxel, WBZ_4 and the JNK inhibitor SP600125 (Calbiochem, Whitehouse Station, NJ) were reconstituted in 100% DMSO. When added to the cells, the final concentration of DMSO on the culture medium was 0.1% or less.

Western blot

Ovarian cancer cells were treated with 10 μM WBZ_4 and collected at various time points. To activate JNK, A2780CP20 cells were seeded on 10-cm plates at 1×10^6 cells/plate. After attaching overnight, cells were treated with 10 μM WBZ_4 or JNK inhibitor SP600125 (Calbiochem) and incubated for 8 hours. Next, medium was removed and saved, and the plates were washed twice with PBS. After the last wash, cells were exposed to 20, 40 and 80J/m^2 of UV light using an FB-UVXL-1000UV crosslinker (Fisher Scientific, Pittsburgh, PA). After a 30 min recovery, cells were harvested and processed for Western blot analysis.

For p-JNK and p-c-JUN, protein lysates were separated on 10% SDS-PAGE gels and blotted onto nitrocellulose membranes (Life Science Research; BioRad, Hercules, CA). Primary antibodies used were: anti p-JNK (Thr183/Tyr185), anti-JNK, anti-p-c-JUN (Ser 61), anti c-JUN (Cell Signaling, Danvers, MA) and anti β-actin monoclonal antibody (Sigma-Aldrich, St. Louis, MO). Secondary antibodies used were: goat HRP anti-rabbit and goat HRP anti-mouse (Cell Signaling).

In vitro cell viability assay

Cells were seeded on 96 well plates at 2×10^3 cells/well and incubated overnight. The next day, cells were treated with different concentrations of WBZ_4 (1, 5, 7.5, 10 and 20 μM), docetaxel (0.005, 0.01 and 0.05 μM) and/or the combination of both drugs and incubated for 72 hr. MTS (Promega, Madison, WI) assay was performed according to the manufacturers instructions. Plates were read at 490 nm in an ELISA plate reader (Kinetic Microplate Reader; Molecular Devices Corp. Sunnyvale, CA). The results are expressed in terms of percent of growth inhibition with respect to the untreated control.

Assessment of cell apoptosis

To determine cell death, cells were plated 24 hr before treating them with 5, 10 and 20 μM of WBZ_4. Cells were incubated further for 72 hr and then collected. FITC Annexin-V and Propidium Iodide (PI) staining was detected by flow cytometry analysis (FACScan/ CellQuest system Becton-Dickinson, San Jose, CA), measuring emission at 530 nm (FL1) and 575 nm (FL3).

Orthotopic tumor implantation

Female athymic nude mice (NCr-nu, 8 to 12 weeks old.) were purchased from Taconic (Hudson, NY, USA). To generate tumors, HeyA8 (3×10^5 cells/0.1 mL HBSS) and A2780-CP20 (1×10^6 cells/0.1 mL HBSS) were injected into the peritoneal cavity of nude mice. Mice (N=10 per group for WBZ_4 experiment and 5 per group for the JNK-siRNA) were monitored for adverse effects of therapy and sacrificed on day 24 or when any of the mice began to appear moribund. Mouse weight, tumor weight, and tumor distribution were recorded.

Therapy experiments in nude mice

To determine the optimal dose of WBZ_4 needed to achieve anti-tumor effects, nude mice bearing HeyA8 tumors were randomly divided into 4 groups (N=10 per group): PBS alone or 75, 150 or 300mg/kg of WBZ_4 by gavage (orally). All therapeutic experiments were started 7 days after tumor cell injection. Once the mice in the control group became moribund (~25 days) mice were sacrificed and the therapeutic effect of the different doses was evaluated in terms of tumor weight and number of nodules. To determine the therapeutic efficacy of WBZ_4 in combination with docetaxel, nude mice bearing HeyA8 or A2780CP20 tumors were randomly divided into 4 groups (N=10 per group): 1) PBS (orally) daily; 2) docetaxel (50 μg/mouse for HeyA8 bearing mice and 35 μg/mouse for the A2780CP20 bearing mice) once a week intraperitoneally (*i.p.*); 3) WBZ_4 (orally) daily; and 4) WBZ_4 (orally) daily plus docetaxel *i.p.* once a week. For comparative studies between WBZ_4 and imatinib, nude mice bearing HeyA8 tumors were randomly split into 6 groups (N=10 per group): 1) vehicle control (PBS); 2) imatinib (50 μg/mouse orally daily); 3) WBZ_4 (orally) daily; 4) 50 μg/mouse docetaxel (*i.p*) once a week; 5) 50 μg/mouse imatinib daily + 50 μg/mouse docetaxel once a week; and 6) WBZ_4 daily + 50 μg/mouse docetaxel once a week.

The therapeutic activity of JNK1 siRNA was evaluated using HeyA8 or SKOV3ip1 tumor cells injected *i.p.* Seven days later, the mice (HEYA8, N=5 and SKOV3ip1, N=10) were randomly assigned to four treatment groups (all treatments were administered *i.p.*): 1) control siRNA-DOPC (5 μg/mouse) twice weekly; 2) control siRNA-DOPC (5 μg/mouse) twice weekly plus docetaxel (50 μg/mouse) once a week; 3) JNK1 siRNA-DOPC (5 μg/mouse) twice weekly; and 4) JNK1 siRNA-DOPC (5μg/mouse) in combination with 50 μg/mouse docetaxel.

SiRNA incorporation into DOPC liposomes

For *in vivo* delivery, the control and JNK1 siRNAs were incorporated into 1,2-Dioleoyl-*sn*-Glycero-3-Phosphocholine (DOPC) liposomes (Avanti Polar Lipids, Alabaster, AL). SiRNA and DOPC were mixed in the presence of excess t-butanol at a ratio of 1:10 (w/w) as described previously (25). After Tween 20 was added, the mixture was frozen in an acetone-dry ice bath, and lyophilized. Before in vivo administration, the lyophilized powder was hydrated with Ca^{2+} and Mg^{2+} free PBS at a concentration of 25 μg/mL to achieve the desired dose in 200 μL/injection.

Immunohistochemistry

Expression of Ki67 and assessment of deoxynucleotidyl transferase-mediated dUTP nick end labeling (TUNEL)-positive cells were determined by immunohistochemical analysis using paraffin-embedded tumors as described previously (26). Ki67 primary antibody (BioCare Medical, Concord, CA) and secondary goat HRP anti-rabbit (Jackson Laboratories, Bar Harbor, ME) were used. Immunohistochemistry for CD31 was done on freshly cut frozen tissue as described before (26). Primary antibody used was anti-CD31

(platelet/endothelial cell adhesion molecule-1, rat IgG; PharMingen). Secondary antibody was goat HRP anti-rat (Jackson Laboratories). Staining was analyzed with 10x objective on a Microphot-FX microscope (Nikon, Garden City, NY) equipped with a three-chip charge-coupled device color video camera (model DXC990, Sony, Tokyo, Japan).

To quantify microvessel density (MVD), 10 random fields at 100x final magnification were examined for each tumor (one slide per mouse, five slides per group) and the number of microvessels per field was counted. To quantify Ki67 expression, the number of positive and negative cells (3,3′-diaminobenzidine staining) was counted in 10 random fields at 100x magnification and the percent of Ki67 positive cells was calculated for each group. To quantify TUNEL positive cells, the number of positive cells was counted in 10 random fields at 100x magnification.

SiRNA transfection

Pre-designed siRNA targeted against JNK1 (S 5′ GGAUGCAAAUCUUUGCCAA [dT] [dT]; AS 5′ UUGGCAAAGAUUUGCAUCC [dT] [dT]) as well as the control siRNA (25) were purchased from Sigma (Sigma-Aldrich). For transfection, cells were seeded on 6 well plates at 8×10^4 cells/well and allowed to attach overnight. The next day, JNK1 and control siRNA were transfected using Lipofectamine 2000 (Invitrogen, Carlsbad, CA) following the manufacturer's instructions. Target downmodulation was confirmed by Western blot. To determine an effect on cell growth and apoptosis, cells were transfected and incubated for 72hr. Next, total cell number was counted and the results expressed as % of growth inhibition or percent of annexin-V positive cells (apoptosis) relative to the untransfected cells.

Analysis of ovarian cancer clinical specimens

One hundred and sixteen epithelial ovarian cancers were obtained at primary debulking surgery and protein was extracted from these tumors as previously described (27-29). The median patient age was 61 years (range, 38-88). Of the 116 tumors, 92 were serous, 5 endometrioid, 3 clear cell and 16 others. Of the tumors, 10 were stage 1, 16 were stage 2, 66 were stage 3, 18 were stage 4 and 6 were unknown for stage. The diagnosis stage was 1 in 10 cases, 2 in 11, 3 in 66 and 4 in 18 cases (remainder unknown) and the tumor was suboptimally debulked in 32 cases. The tumor lysates were subjected to reverse phase protein array (RPPA) with antibodies to JNK (Santa Cruz, Inc. (Santa Cruz, CA) cat. no. 474) and phosphorylated JNK (Cell Signaling, Inc. cat. no. 9251) as previously described (27-29). Note that these antibodies are not JNK isoform-specific. The raw spot signal intensities from quantification of the RPPA slide images were processed by the R package SuperCurve (version 0.997) (30). The protein concentrations for JNK and pJNK were then normalized by loading correction and the data were log2 centered as previously described (27-29). Kaplan-Meier survival curves were used to determine the association between the concentrations of JNK and pJNK and survival endpoints (both progression-free (PFS) and overall survival (OS) times, both measured from the time of debulking surgery). Cox proportional hazards models were applied to clinical and antibody variables that were significantly associated with outcome measures in univariate analysis.

Statistical analysis

For the *in vivo* experiments, differences in continuous variables (mean body weight, tumor weight, MVD, Ki-67 and TUNEL staining) were analyzed using the Student's t test for comparing two groups and by ANOVA for multiple group comparisons with $P < 0.05$ considered statistically significant.

Results

WBZ_4 inhibits JNK basal activity in ovarian cancer cells

We first used Western blot analysis to examine phospho-JNK-1 and 2 and JNK-1 and 2 levels in different ovarian cancer cell lines (S1). Then, we tested the efficacy of WBZ_4 for inhibiting JNK-1 expression in some of those cells. A2780CP20 cells were treated with WBZ_4 (10 μM) and collected at different time points up to 24 hours after the treatment. Untreated cells and cells treated with 0.1% DMSO showed the presence of pJNK1/2 at low levels (Fig 1A). Starved cells given serum shock were used as a positive control for pJNK activation showing indeed an increase in the levels of pJNK1/2. Treatment with WBZ_4 resulted in a sustained decrease in pJNK1/2 levels noticeable as soon as 2 hr after the treatment and lasting for up to 12 hr. No changes were noted in total JNK1/2 levels.

UV induction has been shown to activate JNK phosphorylation as well as that of its downstream targets (1, 4, 31). To determine whether WBZ_4 can block JNK activation, A2780CP20 cells were treated with 10 μM of either WBZ_4 or SP600125 for 8 hr followed by exposure to UV light (20, 40 and 80 J/m^2). Western blot analysis was performed on the cells extracts to assess the levels of both p-JNK and p-c-Jun as indicators of JNK activity (Fig 1B). JNK was readily activated in untreated A2780CP20 cells as shown by increased levels of p-JNK and p-c-Jun. However, at UV levels of 20 and 40 J/m^2, WBZ_4 and SP600125 prevented phosphorylation of both JNK and c-Jun. Particularly, when the UV levels were 40 J/m^2, the addition of WBZ_4 or SP600125 reduced p-JNK levels by 5-fold (p<0.001). Under the same UV levels, the addition of SP600125 or WBZ_4 reduced p-c-Jun levels by 2.5- and 3-fold (p<0.01), respectively (Figure 1C-D). At 80 J/m^2, neither drug was capable of inhibiting JNK activity, suggesting that this high level of UV overrides any type of inhibition occurring in the cells.

WBZ_4 inhibit growth of ovarian cancer cell lines

On the basis of the JNK-1 inhibitory activity of WBZ_4, we next asked whether this inhibitor would affect *in vitro* growth of ovarian cancer cells. Following treatment for 72 hours, dose dependent growth inhibition was observed in all the cell lines tested with IC50 values ranging between 7.5 μM and 15 μM (Fig 2A). In order to assess whether the effects on cell viability were related to apoptosis, FACS analysis after FITC-Annexin V staining was performed. This analysis showed a dose dependent increase in the percentage of cells labeled positively with Annexin V, indicating that the growth inhibition observed was likely a result of cellular apoptosis (Fig 2B). WBZ_4 was originally designed to specifically inhibit c-Kit and JNK-1 to avoid potential cardiotoxicity (21). Given that ovarian cancer cells do not express detectable levels of c-Kit (data not shown), we reasoned that WBZ_4 was most likely functioning via JNK-1 inhibition. The JNK inhibitor SP600125 was used as a positive control. As shown in Figure 2C, ovarian cancer cells treated with increasing concentrations of SP600125 for 72 hr showed dose dependent growth inhibition (IC50 levels between 25 and 30 μM). The IC50s observed with SP600125 were similar to those published for other tumor cell lines (12, 15, 19, 32).

Given the effect established for the SP600125 JNK inhibitor in arresting cells at the G2/M phase of the cell cycle (33), we studied the effects of both, SP600125 and WBZ_4 on cell cycle distribution of the ovarian cancer cells. Treatment of either A2780 or HeyA8 cells with 15 μM of SP600125 led to a decrease in the percentage of cells in the G1 phase and an increase in the cells at the S and G2/M phases of the cell cycle (Fig 2D) in accordance with the published data (20). However, in the HeyA8 cells, WBZ_4 induced a clear increase in the percentage of cells in the SubG1 population (dead cells) at the two concentrations tested (10 and 15 μM), whereas in the A2780CP20 cells, 10 μM of WBZ_4 led to arrest of the

cells at the G2/M. Higher concentrations (15 μM) resulted in an approximately 20% increase in the subG1 population with a concomitant decrease in the percentage of cells at the G1 phase of the cell cycle.

Therapeutic efficacy of WBZ_4

To evaluate *in vivo* the therapeutic effect of the combination of WBZ_4 and docetaxel (34-39), we first performed preliminary dose-response experiments for WBZ_4. Nude mice bearing HeyA8 tumors were treated daily with one of three different doses of WBZ_4 (75, 150 and 300 mg/kg) for approximately three weeks. Assessment of tumor weight and number of nodules at the end of the experiment revealed that the 150 mg/kg dose gave the most consistent results, which was selected for subsequent experiments (S2). The *in vivo* anti-tumor activity of WBZ_4 was determined in nude mice implanted with either HeyA8 or A2780CP20 cells (Fig 3). Seven days later, mice were randomly distributed into four treatment groups: 1) Control: PBS; 2) WBZ_4 (gavage); 3) docetaxel (I.P.) and 4) WBZ_4 (gavage) plus docetaxel (I.P.). The *in vitro* effect of docetaxel in these cell lines alone or in combination with WBZ_4 is shown in S3. In the HeyA8 tumor bearing mice, comparison of the mean tumor weights across different groups revealed that WBZ_4 and docetaxel resulted in a statistically significant reduction in mean tumor weight when compared to the PBS treated mice ($p<0.01$), and this reduction was increased even further when both drugs were combined ($p<0.001$). Each drug alone also induced a statistically significant decrease in the number of nodules ($p<0.05$), which were further decreased when both drugs were combined ($p<0.01$) (Fig 3A). In the A2780CP20 model (Fig 3B), WBZ_4 and the combination of WBZ_4 plus docetaxel were effective in reducing tumor weight compared to controls ($p<0.05$). In this model, each treatment induced a reduction in the number of nodules compared to controls ($p<0.05$ for the combination group).

Since WBZ_4 was redesigned from imatinib, we also asked whether the activity of WBZ_4 is distinct from imatinib against ovarian carcinoma. In the HeyA8 model, treatment with imatinib did not affect tumor growth (Fig 3C). However, WBZ_4 monotherapy reduced tumor growth by 50% ($p=0.03$) and the combination of WBZ_4 and docetaxel reduced tumor growth by 90% ($p<0.001$; Figure 3C). Tumor samples harvested from this experiment confirmed that WBZ_4 reduced the levels of pJNK whereas imatinib had no effect on p-JNK (Fig 3D).

Effect of WBZ_4 therapy on angiogenesis, cell proliferation, and apoptosis

Next, we examined the effects of WBZ_4 therapy on cell proliferation, apoptosis and microvessel density (MVD). WBZ_4 or docetaxel treatment resulted in decreased MVD when compared to controls (Fig 4A), which was further decreased by combination treatment. Cell proliferation was assessed by staining for the nuclear marker Ki-67. WBZ_4 induced a significant decrease in the Ki-67 index ($p<0.05$; Fig 4B) which was decreased further in the combination group ($p<0.001$). Tunel staining showed similar effects on apoptosis in response to therapy (Fig 4C).

JNK1 silencing inhibits cell growth

To confirm that JNK inhibition leads to growth arrest in ovarian cancer cells, we used JNK1 siRNA to specifically target JNK1 in the HEYA8, A2780CP20, SKOV31ip1 and SKOV3.TR ovarian cancer cells (Fig 5). Cells treated with siRNA showed a 60-90% decrease in JNK1 expression compared to the untreated or the control siRNA treated cells (Fig 5A). Compared with control siRNA, a 30-40% reduction in cell growth was observed in the four cell lines tested (Fig 5B). Likewise, FACS analysis indicated that JNK1 siRNA transfection increased apoptosis in the four cell lines tested (Fig 5C).

Therapeutic effect of *in vivo* JNK1 silencing

To determine if JNK1 silencing specifically was responsible for the *in vivo* anti-tumor effects, we utilized JNK1 siRNA incorporated into DOPC nanoliposomes in HeyA8 (N=5) and SKOV3ip1 (N=10)-bearing nude mice according to the following groups: 1) control-siRNA DOPC liposomes; 2) JNK1-siRNA DOPC liposomes; 3) docetaxel + control-siRNA DOPC liposomes; 4) JNK1-siRNA DOPC liposomes + docetaxel. Either JNK1 siRNA-DOPC or docetaxel significantly decreased tumor weight, which was further reduced in the combination group ($p < 0.05$ for HEYA8, Fig 6B; and $p < 0.001$ for SKOV3ip1, Figure 6E). JNK1 siRNA-DOPC also induced a significant decrease in the number of nodules in both HEYA8 ($p < 0.05$, Fig. 6A) and SKOV3ip1 ($p < 0.01$) models. The number of nodules was further decreased in the combination groups (HEYA8 $p < 0.05$, Figure 6A; and SKOV3ip1 $p < 0.001$, Figure 6D).

JNK and pJNK expression in human ovarian carcinoma

Given the paucity of data regarding JNK expression in human ovarian carcinoma, we examined JNK and pJNK in 116 epithelial ovarian cancers obtained at primary debulking surgery by reverse phase protein assay (RPPA). Out of the 116 specimens, 50% (58) showed high levels of pJNK. Low and High expression were simply defined using the mean expression value for pJNK. We found that pJNK was significantly associated with progression free survival (PFS; Fig. 6G), but not with overall survival (OS). JNK expression was not significantly associated with either PFS or OS time. Since both residual disease at debulking surgery and stage at diagnosis were also significantly associated with PFS time, a Cox model for PFS was constructed using pJNK, stage and residual disease. In this model, both residual disease ($p=0.01$) and pJNK ($p=0.04$) remained significant predictors of PFS. When the survival analysis was confined to those with stages 3 or 4 cancer only, PFS was still significant (Supplementary Figure 4). In addition, pJNK was significantly more highly expressed in stage 3 and 4 cases *versus* stage 1 and 2 cases (t test p value = 0.024).

Discussion

The key finding from our study is that activated JNK1 is present in a substantial proportion of ovarian cancers, and is predictive of decreased PFS. Inhibition of JNK-1 in ovarian cancer cells leads to growth inhibition and apoptosis resulting in anti-tumor efficacy in vivo. To inhibit JNK1 activity, we used the newly developed WBZ_4 compound, which suppressed both basal, and UV induced phosphorylation of JNK1 in ovarian cancer cells. WBZ_4 demonstrated even greater therapeutic activity in combination with docetaxel.

JNKs are members of the well known family of MAPKs. Despite the controversial roles described for JNKs in mediating cell death as well as cell survival and tumorogenesis, several lines of evidences support the notion that under basal conditions JNK is necessary to promote progression through the cell cycle and therefore to promote cell proliferation (12-19). JNK was even shown to be necessary for the development of gastric cancer, indicating the tumorigenic potential of this protein and the importance of its inhibition in this model (13). Work done in other models and cell lines arrived to similar conclusions.

Given the role of several kinases in cell survival, proliferation, differentiation, apoptosis and transformation, tyrosine and in general, kinase inhibitors have emerged as strong agents for the treatment of different types of cancers and other diseases (40-41). However, because of the great degree of conservation present across kinases, it is difficult to control specificity of the inhibitors and in many cases, this leads to undesired toxicity (42-43). Here, we used WBZ_4, a compound recently derived from imatinib after applying a new conceptual model in order to curve its activity towards c-Kit and JNK1. We demonstrated earlier that non-

conserved sites among different targets with low water residence time have a higher propensity to dehydrate, therefore called de-wetting hot spots. Given that these hot spots are present in non-conserved residues, they serve as a discriminator among paralogs. Targeting these unique de-wetting hot spots allows for the design of potentially more specific kinase inhibitors (20-21).

Earlier work using this paradigm led to the synthesis of WBZ_4, which indeed was more specific for c-Kit and was able to bind in vitro to c-Jun NH2-terminal Kinase 1 (21), a property absent from the parental compound. Previously, we showed that WBZ_4 is highly effective for the management of gastrointestinal stromal tumors (GIST) due to inhibition of c-Kit activity; however, it does not have any effect on chronic myeloid leukemia where imatinib is widely used. While imatinib lacks activity in ovarian carcinoma, WBZ_4 is highly active. This finding is likely reflective of JNK1 inhibition since ovarian cancers largely lack c-Kit expression. This contention is supported by the fact that JNK1 siRNA-DOPC was able to inhibit tumor growth to an extent that was similar to WBZ_4.

In summary, we demonstrate the functional, clinical and biological significance of JNK-1 in ovarian carcinoma. Moreover, we provide evidence for a novel inhibitor of JNK that merits further clinical development.

Supplementary Material

Refer to Web version on PubMed Central for supplementary material.

Acknowledgments

The authors thank Robert Langley, Donna Reynolds, Yunfang Wang, Nicholas Jennings and the Lopez lab members for helpful discussions and/or technical assistance.

This research was funded in part by NIH grants (CA109298, CA110793, and CA092115), The Marcus Foundation, the U.T.M.D. Anderson Cancer Center SPORE in Ovarian Cancer (P50CA083639), a Program Project Development Grant from the Ovarian Cancer Research Fund, Inc., the Zarrow Foundation, and the Betty Ann Asche Murray Distinguished Professorship.

References

1. Davis RJ. Signal transduction by the JNK group of MAP kinases. Cell. 2000; 103:239–52. [PubMed: 11057897]
2. Harper SJ, LoGrasso P. Signalling for survival and death in neurones: the role of stress-activated kinases, JNK and p38. Cellular signalling. 2001; 13:299–310. [PubMed: 11369511]
3. Chang L, Karin M. Mammalian MAP kinase signalling cascades. Nature. 2001; 410:37–40. [PubMed: 11242034]
4. Hibi M, Lin A, Smeal T, Minden A, Karin M. Identification of an oncoprotein- and UV-responsive protein kinase that binds and potentiates the c-Jun activation domain. Genes & development. 1993; 7:2135–48. [PubMed: 8224842]
5. Kyriakis JM, Banerjee P, Nikolakaki E, et al. The stress-activated protein kinase subfamily of c-Jun kinases. Nature. 1994; 369:156–60. [PubMed: 8177321]
6. Kyriakis JM, Avruch J. Mammalian mitogen-activated protein kinase signal transduction pathways activated by stress and inflammation. Physiological reviews. 2001; 81:807–69. [PubMed: 11274345]
7. Potapova O, Haghighi A, Bost F, et al. The Jun kinase/stress-activated protein kinase pathway functions to regulate DNA repair and inhibition of the pathway sensitizes tumor cells to cisplatin. The Journal of biological chemistry. 1997; 272:14041–4. [PubMed: 9162025]

8. Kuan CY, Yang DD, Roy DR Samanta, Davis RJ, Rakic P, Flavell RA. The Jnk1 and Jnk2 protein kinases are required for regional specific apoptosis during early brain development. Neuron. 1999; 22:667–76. [PubMed: 10230788]
9. Sabapathy K, Hu Y, Kallunki T, et al. JNK2 is required for efficient T-cell activation and apoptosis but not for normal lymphocyte development. Curr Biol. 1999; 9:116–25. [PubMed: 10021384]
10. Sabapathy K, Jochum W, Hochedlinger K, Chang L, Karin M, Wagner EF. Defective neural tube morphogenesis and altered apoptosis in the absence of both JNK1 and JNK2. Mechanisms of development. 1999; 89:115–24. [PubMed: 10559486]
11. Sabapathy K, Hochedlinger K, Nam SY, Bauer A, Karin M, Wagner EF. Distinct roles for JNK1 and JNK2 in regulating JNK activity and c-Jun-dependent cell proliferation. Molecular cell. 2004; 15:713–25. [PubMed: 15350216]
12. Alexaki VI, Javelaud D, Mauviel A. JNK supports survival in melanoma cells by controlling cell cycle arrest and apoptosis. Pigment cell & melanoma research. 2008; 21:429–38. [PubMed: 18541008]
13. Shibata W, Maeda S, Hikiba Y, et al. c-Jun NH2-terminal kinase 1 is a critical regulator for the development of gastric cancer in mice. Cancer research. 2008; 68:5031–9. [PubMed: 18593901]
14. Vivanco I, Palaskas N, Tran C, et al. Identification of the JNK signaling pathway as a functional target of the tumor suppressor PTEN. Cancer cell. 2007; 11:555–69. [PubMed: 17560336]
15. Gross ND, Boyle JO, Du B, et al. Inhibition of Jun NH2-terminal kinases suppresses the growth of experimental head and neck squamous cell carcinoma. Clin Cancer Res. 2007; 13:5910–7. [PubMed: 17908987]
16. Potapova O, Gorospe M, Bost F, et al. c-Jun N-terminal kinase is essential for growth of human T98G glioblastoma cells. The Journal of biological chemistry. 2000; 275:24767–75. [PubMed: 10825181]
17. Potapova O, Gorospe M, Dougherty RH, Dean NM, Gaarde WA, Holbrook NJ. Inhibition of c-Jun N-terminal kinase 2 expression suppresses growth and induces apoptosis of human tumor cells in a p53-dependent manner. Molecular and cellular biology. 2000; 20:1713–22. [PubMed: 10669748]
18. Bost F, McKay R, Dean N, Mercola D. The JUN kinase/stress-activated protein kinase pathway is required for epidermal growth factor stimulation of growth of human A549 lung carcinoma cells. The Journal of biological chemistry. 1997; 272:33422–9. [PubMed: 9407138]
19. Du L, Lyle CS, Obey TB, et al. Inhibition of cell proliferation and cell cycle progression by specific inhibition of basal JNK activity: evidence that mitotic Bcl-2 phosphorylation is JNK-independent. The Journal of biological chemistry. 2004; 279:11957–66. [PubMed: 14704147]
20. Fernandez A, Sanguino A, Peng Z, et al. Rational drug redesign to overcome drug resistance in cancer therapy: imatinib moving target. Cancer research. 2007; 67:4028–33. [PubMed: 17483313]
21. Fernandez A, Sanguino A, Peng Z, et al. An anticancer C-Kit kinase inhibitor is reengineered to make it more active and less cardiotoxic. The Journal of clinical investigation. 2007; 117:4044–54. [PubMed: 18060038]
22. Sood AK, Shahin MS, Sorosky JI. Paclitaxel and platinum chemotherapy for ovarian carcinoma during pregnancy. Gynecologic oncology. 2001; 83:599–600. [PubMed: 11733979]
23. Apte SM, Bucana CD, Killion JJ, Gershenson DM, Fidler IJ. Expression of platelet-derived growth factor and activated receptor in clinical specimens of epithelial ovarian cancer and ovarian carcinoma cell lines. Gynecologic oncology. 2004; 93:78–86. [PubMed: 15047217]
24. Schmandt RE, Bennett M, Clifford S, et al. The BRK tyrosine kinase is expressed in high-grade serous carcinoma of the ovary. Cancer biology & therapy. 2006; 5:1136–41. [PubMed: 16855388]
25. Landen CN Jr. Chavez-Reyes A, Bucana C, et al. Therapeutic EphA2 gene targeting in vivo using neutral liposomal small interfering RNA delivery. Cancer research. 2005; 65:6910–8. [PubMed: 16061675]
26. Halder J, Kamat AA, Landen CN Jr. et al. Focal adhesion kinase targeting using in vivo short interfering RNA delivery in neutral liposomes for ovarian carcinoma therapy. Clin Cancer Res. 2006; 12:4916–24. [PubMed: 16914580]
27. Gonzalez-Angulo AMS-HK, Palla SL, Carey M, Agarwal R, Meric-Bernstam F, Traina TA, Hudis C, Hortobagyi GN, Gerald WL, Mills GB, Hennessy BT. Androgen receptor levels and association with PIK3CA mutations and prognosis in breast cancer. Clinical Cancer Research. 2008 In press.

28. Stemke-Hale K, Gonzalez-Angulo AM, Lluch A, et al. An integrative genomic and proteomic analysis of PIK3CA, PTEN, and AKT mutations in breast cancer. Cancer research. 2008; 68:6084–91. [PubMed: 18676830]
29. Hennessy BT, Lu Y, Poradosu E, et al. Pharmacodynamic markers of perifosine efficacy. Clin Cancer Res. 2007; 13:7421–31. [PubMed: 18094426]
30. Hu J, He X, Baggerly KA, Coombes KR, Hennessy BT, Mills GB. Non-parametric quantification of protein lysate arrays. Bioinformatics (Oxford, England). 2007; 23:1986–94.
31. Ip YT, Davis RJ. Signal transduction by the c-Jun N-terminal kinase (JNK)--from inflammation to development. Current opinion in cell biology. 1998; 10:205–19. [PubMed: 9561845]
32. Ennis BW, Fultz KE, Smith KA, et al. Inhibition of tumor growth, angiogenesis, and tumor cell proliferation by a small molecule inhibitor of c-Jun N-terminal kinase. The Journal of pharmacology and experimental therapeutics. 2005; 313:325–32. [PubMed: 15626722]
33. Oktay K, Buyuk E, Oktem O, Oktay M, Giancotti FG. The c-Jun N-terminal kinase JNK functions upstream of Aurora B to promote entry into mitosis. Cell cycle (Georgetown, Tex. 2008; 7:533–41.
34. Ringel I, Horwitz SB. Studies with RP 56976 (taxotere): a semisynthetic analogue of taxol. J Natl Cancer Inst. 1991; 83:288–91. [PubMed: 1671606]
35. Hsu Y, Sood AK, Sorosky JI. Docetaxel versus paclitaxel for adjuvant treatment of ovarian cancer: case-control analysis of toxicity. Am J Clin Oncol. 2004; 27:14–8. [PubMed: 14758127]
36. Huang S, Van Arsdall M, Tedjarati S, et al. Contributions of stromal metalloproteinase-9 to angiogenesis and growth of human ovarian carcinoma in mice. J Natl Cancer Inst. 2002; 94:1134–42. [PubMed: 12165638]
37. Gueritte-Voegelein F, Guenard D, Lavelle F, Le Goff MT, Mangatal L, Potier P. Relationships between the structure of taxol analogues and their antimitotic activity. J Med Chem. 1991; 34:992–8. [PubMed: 1672159]
38. Barasoain I, De Ines C, Diaz F. Interaction of tubulin and cellular microtubules with Taxotere (RP56976), a new semisynthetic analog of Taxol. Proc Am Assoc Cancer Res. 1991; 32:329.
39. Vasey PA. Preliminary results of the SCOTROC Trial: a phase III comparison of paclitaxel-carboplatin (PC) and docetaxel-carboplatin (DC) as first-line chemotherapy for stage IC-IV epithelial ovarian cancer (EOC). Scottish Gynecologic Cancer Trials Group. Proc of the Am Soc Clin Oncol. 2001
40. Fabian MA, Biggs WH 3rd, Treiber DK, et al. A small molecule-kinase interaction map for clinical kinase inhibitors. Nature biotechnology. 2005; 23:329–36.
41. Tibes R, Trent J, Kurzrock R. Tyrosine kinase inhibitors and the dawn of molecular cancer therapeutics. Annual review of pharmacology and toxicology. 2005; 45:357–84.
42. Druker BJ. Molecularly targeted therapy: have the floodgates opened? The oncologist. 2004; 9:357–60. [PubMed: 15266089]
43. Knight ZA, Shokat KM. Features of selective kinase inhibitors. Chemistry & biology. 2005; 12:621–37. [PubMed: 15975507]

Statement of Translational Relevance

We demonstrate here the functional, clinical and biological significance of JNK-1 in ovarian carcinoma. Moreover, we provide evidence on the mechanisms of action and antitumor effects of a novel inhibitor of JNK that merits further clinical development.

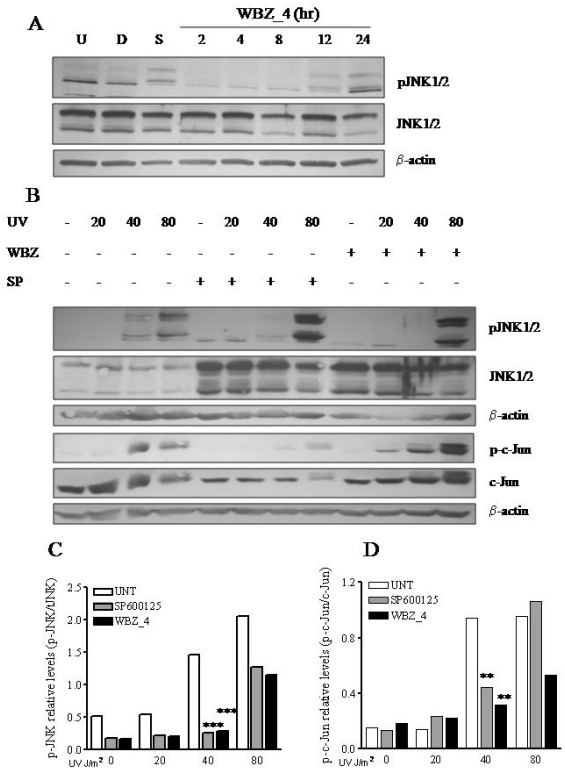

Figure 1.

WBZ_4 inhibits JNK activity in ovarian cancer cells. **A.** Basal p-JNK levels in cells treated with WBZ_4. Protein extracts from A2780CP20 cells treated with 10 μM WBZ_4 and collected at different time points were probed with pJNK, total JNK and β-actin. U, untreated sample; D, vehicle treated sample; S, serum shocked positive control. **B.** UV-dependent JNK activation and c-Jun phosphorylation. Protein extracts from cells treated with 10 μM of WBZ_4 or SP600125 and exposed to UV lights were probed with antibodies against the phosphorylated and total form of JNK and c-Jun. To show equal loading, blots were also probed with β-actin. UV, level of energy in J/m^2; WBZ, WBZ_4; SP, SP600125. **C-D**. Densitometric analysis of blots shown in Figure 1B.

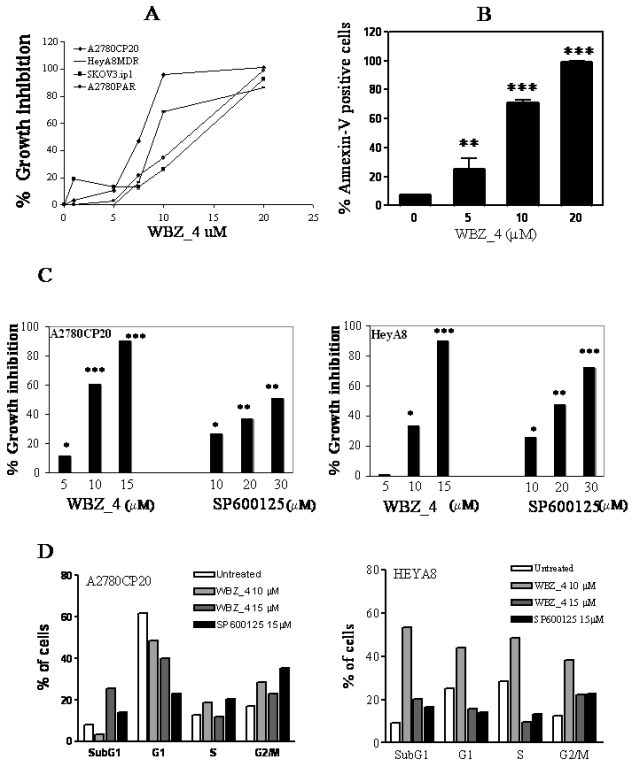

Figure 2.

WBZ_4 and the JNK inhibitor SP600125 inhibit growth of ovarian cancer cells. **A.** Percentage growth inhibition of ovarian cancer cells vs. different concentrations of WBZ_4. Cells were treated with the drug for 72 hr followed by MTS assay. **B.** Percentage of FITC-Annexin V positive cells. A2780CP20 cells were treated with WBZ_4 and 72hr later, Annexin V labeling was assayed by FACS. 5 μM (*p<0.05), 10 μM (***p<0.001) and 20 μM (***p<0.001) **C.** Percentage growth inhibition vs. WBZ_4 and SP600125. Cell viability was assessed by MTS assay 72 hr after treatment. A2780CP20: 5 μM WBZ_4 (*p<0.05), 10 μM WBZ_4 (***p<0.001) and 20 μM WBZ_4 (***p<0.001); 5 μM SP600125 (*p<0.05), 10 μM SP600125 (**p<0.01) and 20 μM SP600125 (**p<0.01). HEYA8: 5 μM WBZ_4 (p>0.05), 10 μM WBZ_4 (*p<0.05) and 20 μM WBZ_4 (***p<0.001); 5 μM SP600125 (*p<0.05), 10 μM SP600125 (**p<0.01) and 20 μM SP600125 (***p<0.001). **D.** Cell cycle distribution of HeyA8 and A2780CP20 cells treated with WBZ_4 and SP600125. Cell cycle was evaluated by FACS based on the PI staining of cells treated with WBZ_4 and SP600125 for 72 hr. Error bars, SEM.

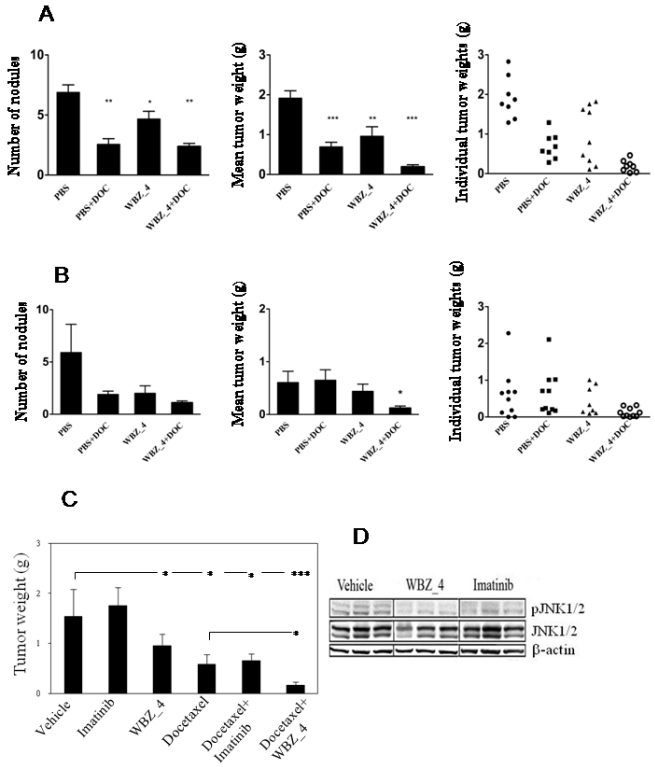

Figure 3.

Therapeutic efficacy of WBZ_4 in combination with docetaxel. HeyA8 **(A)** or A2780CP20 **(B)** cells were implanted intraperitoneally as described in Materials and Methods. Mice were randomly allocated to one of the following groups, with therapy beginning 1week after tumor cell inoculation: PBS, PBS+ docetaxel, WBZ_4 and WBZ_4 + docetaxel. Left columns, number of nodules; center columns, mean tumor weights (bars, SD). Right, individual weights. **C.** WBZ_4 therapeutic activity was compared to that of imatinib in HeyA8 tumor bearing mice. Nude mice were injected i.p. with HeyA8 cells and randomly allocated to one of the following groups, with therapy beginning 1week after tumor cell inoculation: Vehicle, imatinib, WBZ_4, PBS+ docetaxel, WBZ_4 + docetaxel and WBZ_4 + imatinib. **D**. pJNK levels in tumor samples treated with vehicle control, WBZ_4 or imatinib (3 mice per group are shown). * $p<0.05$; ** $p<0.01$; *** $p<0.001$.

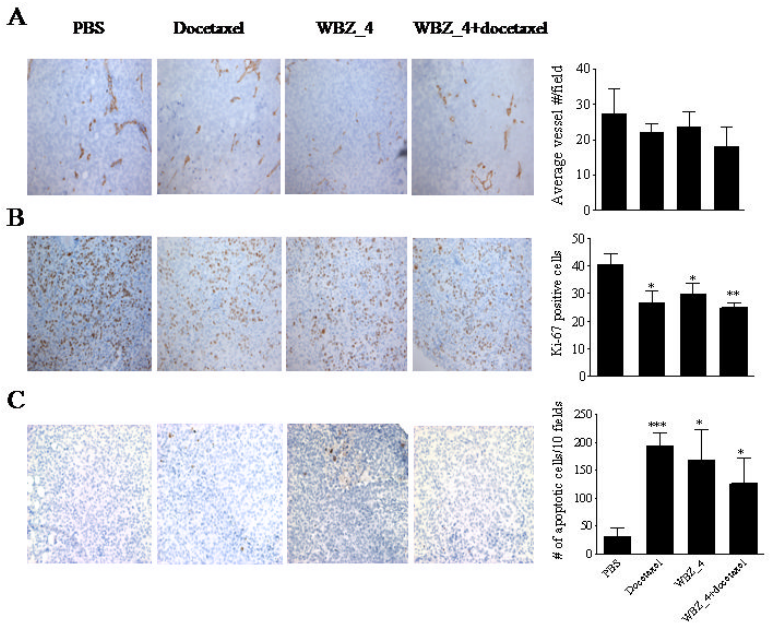

Figure 4.

Effect of WBZ_4 with or without docetaxel on cell proliferation, apoptosis and microvessel density. **A**. MVD was determined after immunohistochemical peroxidase staining for CD31. **B.** Ki67 immunohistochemistry (IHC). Original magnification, 100x. Columns, mean percentage of Ki67-positive cells; bars, SD. Five animals per group and at least five fields per animal were counted. **C.** TUNEL IHC. Tumor sections from each group were stained for TUNEL. Representative slides from each group are shown. The number of apoptotic cells was counted. Columns, mean number of TUNEL-positive cells; bars, SD. Ten fields per slide and at least five slides per group (all from different animals) were counted.

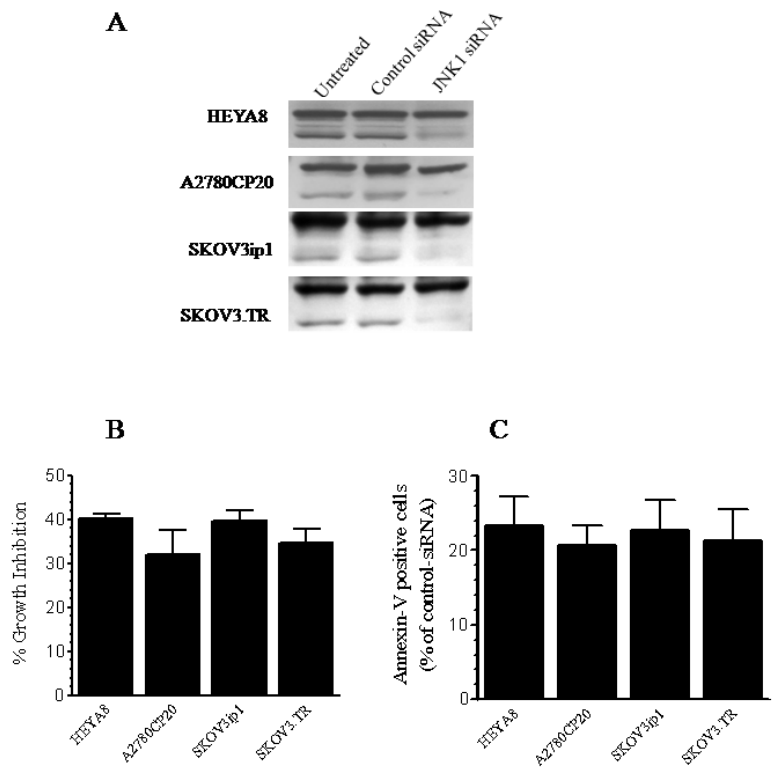

Figure 5.

JNK1 siRNA inhibits growth of ovarian cancer cells. **A.** Effect of JNK1 siRNA on JNK1 expression in different ovarian cancer cells. Western blot of extracts from cells transfected with control and JNK1 siRNA and probed with JNK and β-actin antibodies. **B.** Effect of JNK1siRNA on cell growth. Seventy two hr after transfection, total cell number was counted on the different groups and results are expressed as % growth inhibition relative to the cells transfected with the control siRNA. Error bars, SD. **C.** Cell death after JNK1 silencing. Cells transfected with JNK1 siRNA were stained with FITC Annexin V and PI and cell death was assessed by FACS.

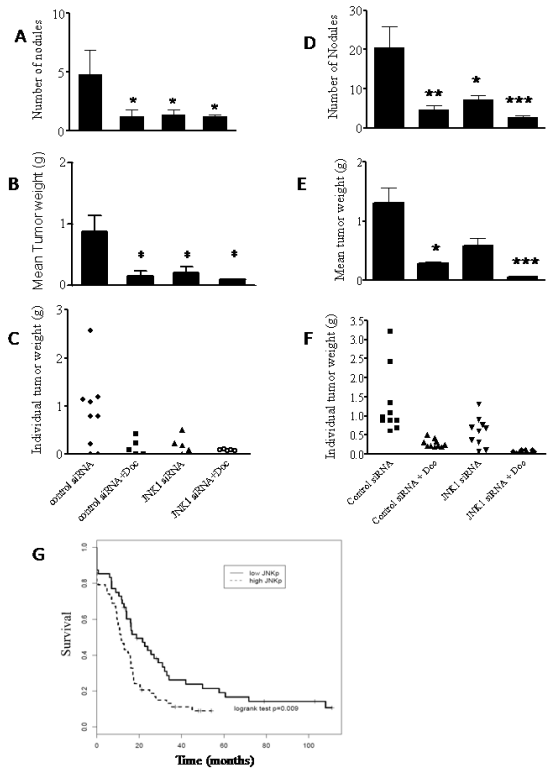

Figure 6.

In vivo therapeutic efficacy of JNK1 siRNA in combination with docetaxel. Nude mice were injected i.p. with HeyA8 (A-C) or SKOV3ip1 (D-F) cells and randomly allocated to one of the following groups, with therapy beginning 1week after tumor cell inoculation: control siRNA DOPC, control siRNA DOPC + Docetaxel, JNK1 siRNA DOPC and JNK1 siRNA DOPC + Docetaxel. Number of nodules (A and D); mean tumor weight (B and E); bars, SD. Individual tumor weights (C and F). G: Kaplan-Meier survival curves for progression free survival (PFS) for all stage tumors based on pJNK (JNKp183_5) levels.